Available online at www.sciencedirect.com
SCIENCE DIRECT®
Carbohydrate Research 338 (2003) 2731–2744
CARBOHYDRATE RESEARCH
www.elsevier.com/locate/carres

Structural profiling of lipopolysaccharide glycoforms expressed by non-typeable *Haemophilus influenzae*: phenotypic similarities between NTHi strain 162 and the genome strain Rd

Elke K.H. Schweda,[a,*] Malin K. Landerholm,[a] Jianjun Li,[b] E. Richard Moxon,[c] James C. Richards[b]

[a] *Clinical Research Centre, Karolinska Institutet and University College of South Stockholm, NOVUM, S-141 86 Huddinge, Sweden*
[b] *Institute for Biological Sciences, National Research Council of Canada, Ottawa, Ontario, Canada K1A OR6*
[c] *Molecular Infectious Diseases Group, Weatherall Institute of Molecular Medicine, University of Oxford Department of Pediatrics, John Radcliffe Hospital, Headington, Oxford 0X3 9DS, UK*

Received 7 April 2003; accepted 13 June 2003

Abstract

Non-typeable *Haemophilus influenzae* (NTHi) is a significant cause of otitis media in children. We have employed single and multiple step electrospray ionization mass spectrometry (ESIMS) and NMR spectroscopy to profile and elucidate lipopolysaccharide (LPS) structural types expressed by NTHi strain 162, a strain obtained from an epidemiological study in Finland. ESIMS on O-deacylated LPS (LPS-OH) and core oligosaccharide (OS) samples of LPS provided information on the composition and relative abundance of glycoforms differing in the number of hexoses linked to the conserved inner-core element, L-α-D-Hep*p*-(1→2)-[*P*Etn→6]-L-α-D-Hep*p*-(1→3)-L-α-D-Hep*p*-(1→5)-[*PP*Etn→4]-α-Kdo*p*-(2→6)-Lipid A of *H. influenzae* LPS. The strain examined was found to elaborate Hex2 to Hex5 LPS glycoform populations having structures identical to those observed for *H. influenzae* strain Rd [Risberg, A.; Masoud, H.; Martin, A.; Richards, J.C.; Moxon, E.R.; Schweda, E.K.H. *Eur. J. Biochem.* **1999**, *261*, 171–180], the strain for which the complete genome has been sequenced. In addition, sialyllactose-containing glycoforms previously identified in strain Rd as well as several NTHi strains, were identified as minor components. Multiple step tandem ESIMS (MS^n) on dephosphorylated and permethylated OS provided information on the arrangement of glycoses within the major population of glycoforms and on the existence of additional isomeric glycoforms. Minor Hex1 and Hex6 glycoforms were detected and characterized where the Hex6 glycoform was comprised of a dihexosamine-containing pentasaccharide chain attached at the proximal heptose residue of the inner-core unit. LPS structural motifs present in the NTHi strain 162 are expressed by a genetically diverse set of disease causing isolates, providing the basis for a vaccine strategy against NTHi otitis media.

Keywords: *Haemophilus*; Lipopolysaccharide; Multiple step tandem mass spectrometry; CE-ESIMS/MS

Abbreviations: LPS, lipopolysaccharide; NTHi, non-typeable *Haemophilus influenzae*; LPS-OH, O-deacylated LPS; Lipid A-OH, O-deacylated lipid A; Kdo, 3-deoxy-D-*manno*-oct-2-ulosonic acid; A*n*Kdo-ol, reduced anhydro Kdo; Hep, L-*glycero*-D-*manno*-heptose; Hex, hexose; HexNAc, *N*-acetylhexosamine; NeuAc, *N*-acetylneuraminic acid; *P*Cho, phosphocholine; *P*Etn, phosphoethanolamine; *PP*Etn, pyrophosphoethanolamine; ESIMS, electrospray ionization mass spectrometry; CE, capillary electrophoresis; MS/MS, tandem mass spectrometry; MS^n, multiple step tandem mass spectrometry; HPAEC, high-performance anion-exchange chromatography.

* Corresponding author. Tel.: +46-8-58583823; fax: +46-8-58583820.
E-mail address: elke.schweda@kfc.ki.se (E.K.H. Schweda).

0008-6215/03/$ - see front matter © 2003 Elsevier Ltd. All rights reserved.
doi:10.1016/S0008-6215(03)00385-9

1. Introduction

Acapsular or non-typeable *Haemophilus influenzae* (NTHi) comprises the majority of *H. influenzae* strains in the human nasopharynx and is a leading cause of otitis media and upper respiratory tract diseases. Otitis media is a common childhood disease which accounts for the highest frequency of pediatric visits in the United States.[1] NTHi has recently been found to be the most frequent pathogen in children with recurrent episodes of acute otitis media and possibly accounts for an increased proportion of cases in children who have received the pneumococcal conjugate vaccine.[2] Glycoconjugate vaccines based on the specific capsular polysaccharide of type b *H. influenzae* have proven successful in the control of invasive *H. influenzae* type b disease in infants. Nevertheless, these vaccines do not provide protection against diseases caused by NTHi because they are only protective against infections caused by *H. influenzae* strains bearing the type b capsule. Potential vaccine candidates to protect against NTHi disease include outer membrane proteins, pili and lipopolysaccharide (LPS).

Cell wall LPS is an essential and characteristic surface component of *H. influenzae* and is implicated as a major virulence factor. *H. influenzae* elaborates short-chain LPS which lacks O-specific polysaccharide chains and is often referred to as lipooligosaccharide. LPS of *H. influenzae* can mimic host glycolipids and has a propensity for reversible antigenic variation. The availability of the complete genome sequence of *H. influenzae* strain Rd[3] has facilitated a comparative study of LPS biosynthetic loci from several capsulated [4] and acapsulated[5] strains. Gene functions have been identified in those strains that are responsible for most of the steps in the biosynthesis of the oligosaccharide portions of the LPS molecules. The biosynthesis of certain outer-core oligosaccharide epitopes of *H. influenzae* LPS is known to be subject to high-frequency on-off switching through a process of phase variation that results in a heterogeneous population of LPS molecules within a single strain.[6] Phase variation is thought to provide an adaptive mechanism which is advantageous for survival of bacteria confronted by the differing microenvironments and immune responses of the host.[7,8] A genetic mechanism contributing to LPS phase variation has been identified in at least five chromosomal loci important in the biosynthesis of outer-core region of *H. influenzae* LPS,[9–11] while the genes responsible for the assembly of the inner-core would appear to be constitutively expressed.[4,5] The inner-core of *H. influenzae* LPS has been found to consist of the triheptosyl oligosaccharide moiety, L-α-D-Hep*p*-(1→2)-[*P*Etn→6]-L-α-D-Hep*p*-(1→3)-[β-D-Glc*p*-(1→4)]-L-α-D-Hep*p*-(1→5)-α-Kdo*p*, in which each of the three heptose residues can provide a point for elongation by oligosaccharide chains or for attachment of non-carbohydrate substituents.[12] *H. influenzae* strains expressing LPS glycoform populations having biantennary[12–16] and triantennary[17–21] structures have been reported.

Our ongoing studies have focused on identifying structural conservation and diversity of LPS expression and the genetic basis for expression and pathogenesis in a representative set of clinical isolates of NTHi obtained from otitis media patients.[5,12–14,16,19–25] These clinical isolates have been characterized by ribotyping and span an *H. influenzae* species-level dendrogram comprising >400 strains of both typeable and NTHi strains.[26] Mass spectrometry has become an increasingly important tool to investigate LPS glycoforms in heterogeneous mixtures for their abundance, composition and sequence. A strategy involving the use of multistage electrospray ionization MS/MS (ESIMS^n) on dephosphorylated and permethylated oligosaccharides[16,27,28] has proved particularly informative for profiling glycoform expression. Here we report structural profiles of glycoform expression in NTHi strain 162 using sensitive MS and detailed NMR techniques. The strain examined expresses populations of glycoforms that are present in strain Rd and other NTHi strains.[12–14,16] In an earlier study, we reported on the location of Gly in the inner-core region of a major Hex2 glycoform.[29] In the present investigation, NTHi 162 was found to elaborate an LPS inner-core structural unit which provides a template for display of biantennary structures from the proximal and distal heptose residues. This structural motif is present in a majority of NTHi strains.

2. Experimental

2.1. Bacterial cultivation and preparation of LPS

NTHi strain 162 was selected from a collection of 107 otitis media isolates (kindly provided by the Finnish Otitis Media Study Group).[13] This strain was chosen for structural analysis as a part of a genetically distinct set obtained from population analysis of *H. influenzae* strains using ribotyping.[26] Bacteria were grown in brain heart infusion (BHI) broth (Difco) (3.7%, w/v) containing nicotinamide adenine dinucleotide (NAD; 2 μg/mL), hemin (10 μg/mL) and neuraminic acid (NeuAc; 10 μg/mL) at 37 °C. Bacteria were harvested and the LPS extracted from lyophilized bacteria by using the phenol–chloroform–petroleum ether method involving precipitation of the LPS with, diethyl ether–acetone (6 vol) as described earlier.[19]

2.2. Chromatography

Gel permeation chromatography (GPC) was performed using a Bio-Gel P4 column (2.6 × 140 cm) with pyridi-

nium acetate (0.05 M, pH 4.5) as eluent. Column eluents were monitored by using a differential refractometer. Gas liquid chromatography (GLC) was carried out using a Hewlett–Packard 5890 instrument with a DB-5 fused silica capillary column [25 m × 0.25 mm (0.25 μm i.d.)] and a temperature gradient of 160 (1 min) → 250 °C at 3 °C/min.

2.3. Preparation of oligosaccharides

2.3.1. O-Deacylation of LPS with hydrazine. O-Deacylation of LPS was achieved as previously described.[30] Briefly, LPS (5 mg) was mixed with anhyd hydrazine (0.5 mL) and stirred at 37 °C for 1 h. The reaction mixture was cooled and cold acetone (5 mL) was added to destroy excess hydrazine. The precipitated O-deacylated LPS (LPS-OH) was centrifuged (48,200*g*, 20 min), the pellet was washed twice with cold acetone, once with diethyl ether, and, then dissolved in water followed by lyophilization.

2.3.2. Mild acid hydrolysis of LPS. Core oligosaccharide fractions were obtained from LPS (50 mg) following mild acid hydrolysis (1% AcOH, pH 3.1, 100 °C, 2 h). The insoluble lipid A (16.2 mg) was separated from the carbohydrate-containing supernatant by centrifugation. The reducing agent, borane-*N*-methylmorpholine complex (11 mg), was included in the hydrolysis mixture, and, following purification by GPC on the Bio-Gel P4 column, two major oligosaccharide fractions, OS-1 (2.5 mg) and OS-2 (6.1 mg) were obtained, which were investigated in this study.

2.3.3. Dephosphorylation. In separate experiments, OS-1 and OS-2 (1 mg each) were stirred with 48% hydrogen fluoride (0.2 mL) for 48 h at 4 °C. Samples were then placed into an ice bath and HF was evaporated under a stream of N_2 to give OS-1HF and OS-2HF, respectively, which were dissolved in water and lyophilised.

2.4. Analytical methods

Sugars were identified as their alditol acetates as previously described.[31] Methylation analysis of intact LPS was accomplished on acetylated material which was obtained by treating the sample with acetic anhydride (0.5 mL) and 4-diethylaminopyridine (0.5 mg) at room temperature for 4 h. Permethylation of OS-1HF and OS-2HF was done without the peracetylation step. Methylation was performed with methyl iodide in Me_2SO in the presence of lithium methylsulfinylmethanide.[32] The methylated oligosaccharides were recovered using a SepPak C18 cartridge and subjected to sugar analysis or sequential analysis by multiple step tandem MS (ESIMS^n). The relative proportions of the various alditol acetates and partially methylated alditol acetates obtained in sugar- and methylation analyses, discussed below, correspond to the detector response of the GLC–MS. The absolute configuration of glycoses was determined by the method devised by Gerwig et al.[33]

2.5. Mass spectrometry

Electrospray ionization mass spectrometry (ESIMS) was performed with a VG Quattro triple quadrupole mass spectrometer (Micromass, Manchester, UK) in the negative ion mode. LPS-OH and OS samples were dissolved in 1:1 water/acetonitrile. Sample solutions were injected via a syringe pump into the running eluent 1:1 water–MeCN at a flow rate of 10 μL/min. ESIMS^n experiments were performed on a Finnigan LCQ iontrap mass spectrometer (Finnigan-MAT, San Jose, CA). Samples were dissolved in 1 mM NaOAc in 70% MeOH–30% water. The applied flow rate was 10 μL/min. All experiments were in the positive ion mode. CE-ESIMS and CE-ESIMS/MS was carried out with a Crystal Model 310 CE instrument (AYI Unicam, Boston, MA, USA) coupled to an API 3000 mass spectrometer (Perkin–Elmer/Sciex, Concord, Canada) via a MicroIonspray interface as described previously.[20] GLC–MS was carried out with a Delsi Di200 chromatograph equipped with a NERMAG R10-10H quadrupole mass spectrometer using the same conditions for GLC as described above.[20]

2.6. NMR spectroscopy

NMR spectra were recorded for solutions in deuterium oxide at 25 °C. Spectra were acquired on a JEOL Esquire 500 spectrometer using standard pulse sequences for two-dimensional (2D) COSY, TOCSY, and NOESY experiments. Mixing times of 50 and 180 ms were used for 500 MHz 2D TOCSY experiments. The mixing time used in the 500 MHz 2D NOESY experiment was 400 ms. ^{1}H NMR chemical shifts are reported in ppm, referenced to internal sodium 3-trimethylsilylpropanoate-d_4 (δ 0.00).

3. Results

3.1. Isolation and characterization of LPS

H. influenzae non-typeable strain 162 is a clinical isolate gathered as a part of a Finnish study of otitis media. The strain was grown in liquid culture and the LPS was isolated by phenol–chloroform–light petroleum extraction. Compositional analysis of the LPS samples showed D-glucose (Glc), D-galactose (Gal), 2-amino-2-deoxy-D-glucose (GlcN), 2-amino-2-deoxy-D-galactose (GalN) and L-*glycero*-D-*manno*-heptose (Hep) in the ratios of 1.0:0.8:0.4:0.1:1.3 which were identified by GLC–MS of

the derived alditol acetates and 2-butyl glycoside derivatives. In addition, in earlier studies the LPS was shown by high-performance anion-exhange chromatography (HPAEC) to contain glycine and *N*-acetyl neuraminic acid (NeuAc).[29,34] Methylation analysis of LPS revealed the presence of terminal Glc, terminal Gal, 4-substituted Gal, 4-substituted Glc, 3-substituted Gal, 2-substituted-Hep, 3,4-disubstituted Hep, terminal GalN and 6-substituted GlcN (Table 1). The data are consistent with biantennary structures, containing the common inner-core element, L-α-D-Hep*p*-(1→2)-L-α-D-Hep*p*-(1→3)-[β-D-Glc*p*-(1→4)]-L-α-D-Hep*p*-(1→5)-α-Kdo*p* of *H. influenzae* LPS linked to the conserved lipid A consisting of a β-(1→6)-linked D-glucosamine disaccharide.[12]

O-Deacylation of LPS by treatment with anhydrous hydrazine under mild conditions afforded a water-soluble material which was subjected to analysis by mass spectrometric techniques. The ESIMS spectrum of the sample obtained in the negative mode revealed abundant molecular peaks corresponding to triply and quadruply charged ions. The MS data (Table 2) pointed to the presence of glycoforms in which each molecular species contains the conserved phosphoethanolamine-substituted triheptosyl inner-core moiety attached via a phosphorylated Kdo linked to the O-deacylated lipid A. As observed earlier, populations of glycoforms were observed which differed by 123 Da (i.e., a *P*Etn group) which was consistent with either phosphate or pyrophosphoethanolamine (*PP*Etn) substitution at the O-4 position of the Kdo residue.[18,12] In the spectrum abundant quadruply charged ions at *m/z* 609.6, 640.3, 741.1 and 772.0, together with the corresponding triply charged ions at *m/z* 812.8, 854.1, 988.5 and 1029.8 indicated the presence of glycoforms with the respective compositions *P*Cho•Hex_2•Hep_3•*P*Etn_1•*P*•Kdo•Lipid A-OH, *P*Cho•Hex_2•Hep_3•*P*Etn_2•*P*•Kdo•Lipid A-OH, *P*Cho•HexNAc•Hex_4•Hep_3•*P*Etn_1•*P*•Kdo•Lipid A-OH and *P*Cho•HexNAc•Hex_4•Hep_3•*P*Etn_2•*P*•Kdo•Lipid A-OH. In addition, minor ions corresponding to Hex3 and Hex4 glycoforms were observed (Table 2). A minor quadruply charged ion at *m/z* 723.0 was observed which was attributed to a sialylated Hex3 glycoform with the composition NeuAc•*P*Cho•Hex_3•Hep_3•*P*Etn_1•*P*•Kdo•Lipid A-OH. Although of low abundance, the presence of sialylated glycoforms could be confirmed in a precursor ion monitoring tandem MS experiment by scanning for loss of *m/z* 290 (NeuAc) following on-line separation by capillary electrophoresis (CE-ESIMS/MS). The resulting spectrum revealed minor quadruply charged ions at *m/z* 723 and 754 corresponding to the glycoforms NeuAc•*P*Cho•Hex_3•Hep_3•*P*$Etn_{1,2}$•P_1•Kdo_1•Lipid A-OH. In this experiment, major ions at *m/z* 796 and 827 were observed corresponding to disialylated Hex3 glycoforms having the respective compositions, $NeuAc_2$•*P*Cho•Hex_3•Hep_3•*P*$Etn_{1,2}$•P_1•Kdo_1•Lipid I A-OH. Fragmentation of the ions at *m/z* 796 and 827 in MS/MS experiments, afforded, inter alia, a fragment ion at *m/z* 581 indicating a NeuAc disaccharide unit in the corresponding glycoforms.

3.2. Characterisation of major core oligosaccharide fractions

Partial acid hydrolysis of LPS with dilute acetic acid afforded an insoluble lipid A and core oligosaccharide fractions which were separated by GPC (see Section 2)

Table 1
Linkage analysis data for LPS derived samples from *H. influenzae* NTHi strain 162

Methylated sugar [a]	T_{gm} [b]	Relative detector response			Linkage assignment
		LPS	OS-1HF [c]	OS-2HF [c]	
2,3,4,6-Me_4-Glc	1.00	17	10	22	D-Glc*p*-(1-
2,3,4,6-Me_4-Gal	1.04	2	6	4	D-Gal*p*-(1-
2,3,6-Me_3-Gal	1.16	8	9	3	-4)-D-Gal*p*-(1-
2,3,6-Me_3-Glc	1.18	17	16	6	-4)-D-Glc*p*-(1-
2,4,6-Me_3-Gal	1.20	13	14	2	-3)-D-Gal*p*-(1-
2,3,4-Me_3-Gal	1.25		1		-6)-D-Gal*p*-(1-
3,4,6,7-Me_4-Hep	1.43	28	32	38	-2)-L,D-Hep*p*(1-
2,6,7-Me_3-Hep	1.49	13	4	24	-3,4)-L,D-Hep*p*-(1-
2,3,4,6-Me_4-GalN	1.55	1	6		D-Gal*p*NAc(1-
2,3,6,-Me_3-GlcN	1.60		1		-4)-D-Glc*p*NAc(1-
3,4,7-Me_3-Hep	1.63		1	1	-2,6)-L,D-Hep*p*-(1-
2,3,4,-Me_3-GlcN	1.68	1			-6)-D-Glc*p*NAc(1-

[a] 2,3,4,6-Me_4-Glc represents 1,5-di-*O*-acetyl-2,3,4,6-tetra-*O*-methyl-D-glucitol-1-d_1, etc.
[b] Retention times (T_{gm}) are reported relative to 2,3,4,6-Me_4-Glc.
[c] OS treated with aq HF prior to methylation analysis.

Table 2
Negative ion ESIMS data and proposed compositions for O-deacylated LPS (LPS-OH) and oligosaccharide preparations OS-1 and OS-2 of non-typeable *H. influenzae* strain 162

Sample	Observed ions (*m/z*)			Molecular mass (Da)		Relative abundance (%)	Proposed composition
	$[M-4H]^{4-}$	$[M-3H]^{3-}$	$[M-2H]^{2-}$	Observed	Calculated		
LPS-OH	609.6	812.8		2441.9	2442.2	28	*P*Cho•Hex_2•Hep_3•*P*Etn_1•P_1•Kdo_1•Lipid A-OH
	640.3	854.1		2565.3	2565.3	37	*P*Cho•Hex_2•Hep_3•*P*Etn_2•P_1•Kdo_1•Lipid A-OH
	tr [a]	866.9		2603.7	2604.3	4	*P*Cho•Hex_3•Hep_3•*P*Etn_1•P_1•Kdo_1•Lipid A-OH
	681.3	908.3		2728.5	2727.3	4	*P*Cho•Hex_3•Hep_3•*P*Etn_2•P_1•Kdo_1•Lipid A-OH
	tr[b]	921.0		2766.0	2766.3	1	*P*Cho•Hex_4•Hep_3•*P*Etn_1•P_1•Kdo_1•Lipid A-OH
	721.4	961.9		2889.2	2889.4	3	*P*Cho•Hex_4•Hep_3•*P*Etn_2•P_1•Kdo_1•Lipid A-OH
	723.0	nd [c]		2895.5	2895.6	1	NeuAc•*P*Cho•Hex_3•Hep_3•*P*Etn_1•P_1•Kdo_1•Lipid A-OH
	741.1	988.5		2968.5	2969.5	7	*P*Cho•$HexNAc_1$•Hex_4•Hep_3•*P*Etn_1•P_1•Kdo_1•Lipid A-OH
	772.0	1029.8		3092.2	3092.5	15	*P*Cho•$HexNAc_1$•Hex_4•Hep_3•*P*Etn_2•P_1•Kdo_1•Lipid A-OH
OS-1			704.4	1410.8	1411.1	2	*P*Cho•Hex_2•Hep_3•*P*Etn_1•*An*Kdo-ol
			733.0	1468.0	1468.2	3	*P*Cho•Gly•Hex_2•Hep_3•*P*Etn_1•*An*Kdo-ol
			785.4	1572.8	1573.3	3	*P*Cho•Hex_3•Hep_3•*P*Etn_1•*An*Kdo-ol
			814.8	1631.6	1630.4	1	*P*Cho•Gly•Hex_3•Hep_3•*P*Etn_1•*An*Kdo-ol
			866.4	1734.8	1735.4	5	*P*Cho•Hex_4•Hep_3•*P*Etn_1•*An*Kdo-ol
			895.1	1792.2	1792.5	2	*P*Cho•Gly•Hex_4•Hep_3•*P*Etn_1•*An*Kdo-ol
			968.0	1938.0	1938.6	61	*P*Cho•HexNAc•Hex_4•Hep_3•*P*Etn_1•*An*Kdo-ol
			989.3	1980.6	1981.0	4	*P*Cho•Ac•HexNAc•Hex_4•Hep_3•*P*Etn_1•*An*Kdo-ol
			996.6	1995.2	1995.7	15	*P*Cho•Gly•HexNAc•Hex_4•Hep_3•*P*Etn_1•*An*Kdo-ol
			1017.3	2036.6	2937.7	4	*P*Cho•Ac•Gly•HexNAc•Hex_4•Hep_3•*P*Etn_1•*An*Kdo-ol
OS-2			704.4	1410.8	1411.1	74	*P*Cho•Hex_2•Hep_3•*P*Etn_1•*An*Kdo-ol
			733.0	1468.0	1468.2	6	*P*Cho•Gly•Hex_2•Hep_3•*P*Etn_1•*An*Kdo-ol
			753.5	1509.0	1510.2	4	*P*Cho•Ac•Gly• Hex_2•Hep_3•*P*Etn_1•*An*Kdo-ol
			785.4	1572.8	1573.3	8	*P*Cho•Hex_3•Hep_3•*P*Etn_1•*An*Kdo-ol
			866.4	1734.8	1735.4	4	*P*Cho•Hex_4•Hep_3•*P*Etn_1•*An*Kdo-ol
			885.6	1773.2		3	n.r.[d]
			967.9	1937.8	1938.6	3	*P*Cho•HexNAc•Hex_4•Hep_3•*P*Etn_1•*An*Kdo-ol

Average mass units were used for calculation of molecular weight values based on proposed compositions as follows: Hex, 162.14; HexNAc, 203.19; Hep, 192.17; Kdo, 220.18; *An*Kdo-ol, 222.20; *P*, 79.98; *P*Etn, 123.05, *P*Cho, 165.13; NeuAc, 291.26; Ac, 42.04; Gly, 57.05 and Lipid A-OH, 953.02. Relative abundance was estimated from the area of the ions relative to the total area (expressed as percentage). Signals representing less than 5% of the base peak are not included in the table.

[a] tr, traces of an ion at *m/z* 650.0.

[b] tr, traces of an ion at *m/z* 690.9.

[c] nd, not detected.

[d] n.r., not rationalized.

to give two major fractions, OS-1 and OS-2. The ESIMS spectrum of OS-1 (see Table 2) showed one major doubly charged ion at *m/z* 968.0 corresponding to a Hex5 glycoform with the composition *P*Cho•HexNAc•Hex_4•Hep_3•*P*Etn_1•*An*Kdo-ol. In addition, minor ions corresponding to Hex2, Hex3 and Hex4 glycoforms were observed. The ESIMS spectrum of OS-2 was dominated by the ion at *m/z* 704.4 which corresponded to a major Hex2 glycoform with the composition *P*Cho•Hex_2•Hep_3•*P*Etn_1•*An*Kdo-ol. All ions in OS-1 and OS-2 showed additional ions corresponding to glycine-substituted species. Minor ions corresponding to acetylated Hex5 and Hex2 glycoforms were observed in OS-1 and OS-2, respectively.

OS-1 and OS-2 were subjected to 48% HF to give OS-1HF and OS-2HF. The methylation analysis data for these are presented in Table 1. Methylation analysis of OS-1HF showed terminal Glc, terminal Gal, 4-substituted Gal, 4-substituted Glc, 3-substituted Gal, terminal GalNAc, 2-substituted Hep and 3,4-disubstituted Hep as the major sugar components. Methylation analysis of OS-2HF revealed mainly terminal Glc, 2-substituted Hep and 3,4-disubstituted Hep.

3.2.1. ESIMS^n analysis of permethylated OS-1HF and OS-2HF. OS-1HF and OS-2HF were permethylated and analyzed by ESIMS^n in order to determine the arrangement of glycoses within glycoforms. The resulting ESIMS spectra obtained in the positive mode are shown in Fig. 1 and summarized in Table 3. Sodiated molecular ions corresponding to the Hex2, Hex3, Hex4 and Hex5 glycoforms identified by ESIMS in OS-1 and OS-2 (Table 2) were observed. In addition, minor ions at *m/*

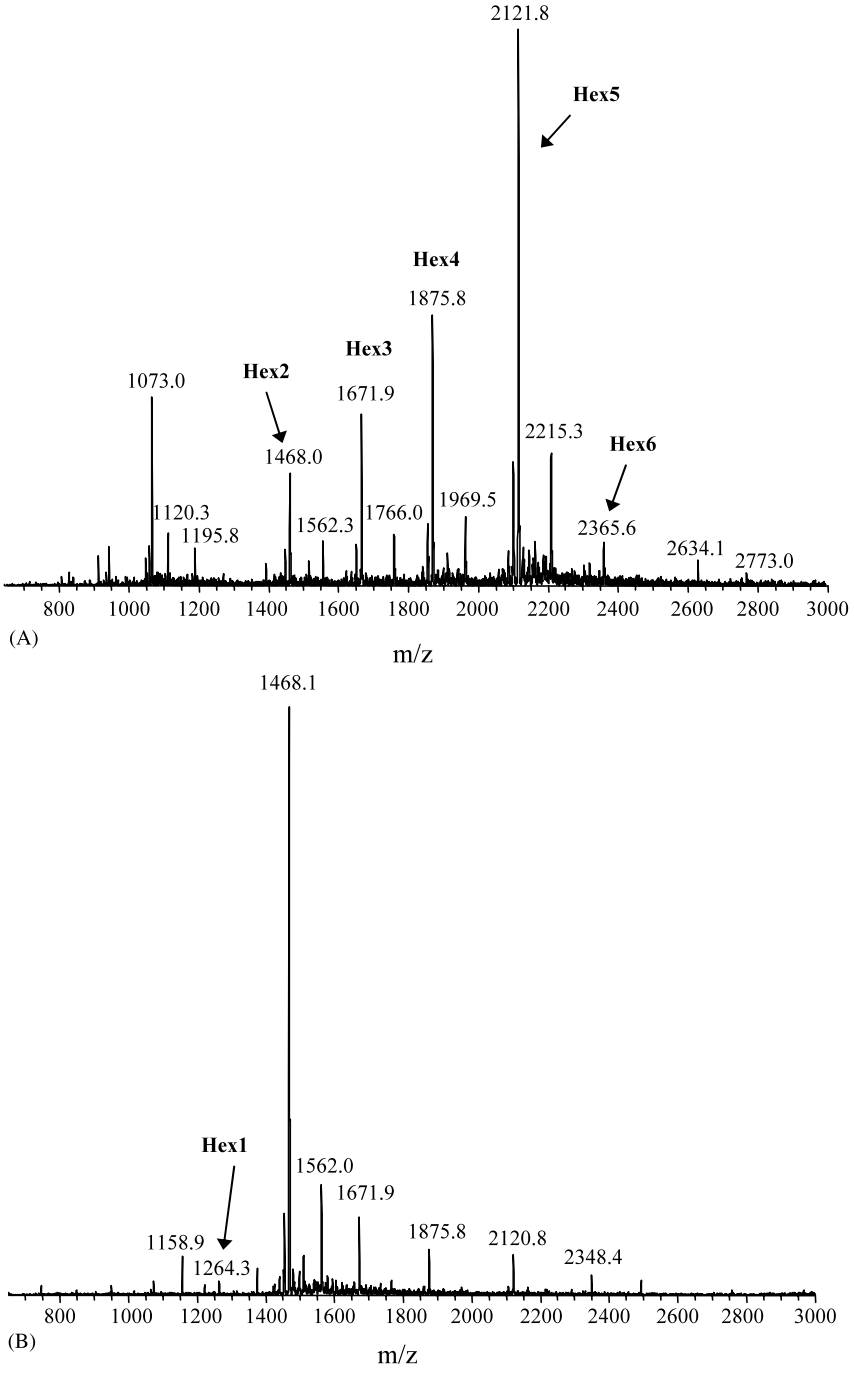

Fig. 1. Parent ion mass spectra (positive mode) of dephosphorylated and permethylated OS-1 (A), and OS-2 (B). Ions corresponding to $[M+Na]^+$ of the Hex1 to Hex6 glycoforms are indicated.

Table 3
Positive ion ESIMS data and proposed compositions for glycoforms of permethylated OS-1HF and OS-2HF

Sample	$[M+Na]^+$	Molecular mass (Da)		Proposed composition	Glycoform
		Observed	Calculated		
OS-1	1468.1	1445.1	1444.5	$Hex_2{\bullet}Hep_3{\bullet}$*An*Kdo-ol	Hex2
	1672.0	1649.0	1648.7	$Hex_3{\bullet}Hep_3{\bullet}$*An*Kdo-ol	Hex3
	1875.9	1852.9	1852.9	$Hex_4{\bullet}Hep_3{\bullet}$*An*Kdo-ol	Hex4
	2121.6	2098.6	2098.2	$HexNAc_1{\bullet}Hex_4{\bullet}Hep_3{\bullet}$*An*Kdo-ol	Hex5
	2365.6	2342.6	2343.5	$HexNAc_2{\bullet}Hex_4{\bullet}Hep_3{\bullet}$*An*Kdo-ol	Hex6
OS-2 [a]	1264.3	1241.3	1240.3	$Hex_1{\bullet}Hep_3{\bullet}$*An*Kdo-ol	Hex1

Average mass units were used for calculation of molecular weight values based on proposed compositions as follows: Hex, 162.14; HexNAc, 203.19; Hep, 192.17; *An*Kdo-ol, 222.20; Me, 14.03; Na, 22.99. All ions showed addition of 94.6 Da which are attributed to uncomplete dephosphorylation.

[a] In addition to a Hex1 glycoform, OS-2 contained all ions as OS-1 except those corresponding to the Hex6 glycoform.

z 1264.3 and 2365.6 corresponding to Hex1 and Hex6 glycoforms with respective compositions $Hex_1{\bullet}Hep_3{\bullet}$*An*Kdo-ol and $HexNAc_2{\bullet}Hex_4{\bullet}Hep_3{\bullet}$*An*Kdo-ol could be detected in this experiment. MS^2 experiments were performed on all molecular ions and in some cases further fragmentation (MS^3) was employed. The obtained data is summarized in Table 4 and structural implications are given in Table 5. One isomeric Hex1 glycoform was defined by ions *m*/*z* 1001.6 and 753.5 corresponding to loss of a terminal Hep-Hep unit from the parent ion (Scheme 1). The other isomeric Hex1 glycoform with a monosubstituted HepI residue was defined by ions *m*/*z* 797.4 and 737.4 due to losses of terminal Hex-Hep and Hep-*An*Kdo-ol units, respectively. This structural conclusion was corroborated by ion *m*/*z* 270.9 observed in the MS^3 experiment ($1264.3 \rightarrow 737.4 \rightarrow$) corresponding to a loss of a terminal Hex-Hep unit as shown in Scheme 1. For the Hex2 glycoform a major isomeric form was identified, the structure of which was in agreement with that reported earlier.[29] It was defined by ions *m*/*z* 1001.6, 753.5 and 737.5 due to losses of terminal Hex-Hep, Hex-Hep-Hep and Hex-Hep-*An*Kdo-ol units, respectively. In conjunction with the ESIMS data of OS-2 and methylation analysis data of OS-2HF, structure **1** could be concluded for the Hex2 OS-2 glycoform.

*P*Cho
↓
β-D-Glc*p*-(1→4)-L-α-D-Hep*p*-(1→5)-*An*Kdo-ol
3
↑
1
L-α-D-Hep*p*6←*P*Etn
2
↑
1
β-D-Glc*p*-(1→2)-L-α-D-Hep*p*

1

Similarly, the Hex3 glycoform was defined by ions *m*/*z* 1001.6, 753.5 and 941.5.4 due to losses of terminal Hex-Hex-Hep, Hex-Hex-Hep-Hep and Hex-Hep-*An*-Kdo-ol (Fig. 2). The ion *m*/*z* 693.4 corresponded to the loss of a branched Hex-Hep(Hep)-*An*Kdo-ol unit. Data obtained by MS^3 experiments ($1672.0 \rightarrow 1249.7 \rightarrow$; $1672.0 \rightarrow 941.5 \rightarrow$) were in agreement with this and no ions indicating branching at HepII were observed. By analogy, tandem MS experiments gave evidence for the Hex4 and Hex5 glycoform structures showing elongation from HepI and HepIII, only.

OS-1 contained minor amounts of a Hex6 glycoform with the composition $HexNAc_2{\bullet}Hex_4{\bullet}Hep_3{\bullet}$*An*Kdo-ol. In this structure, it was evident that HepIII was elongated by one hexose unit from the ion *m*/*z* 1900.6 (loss of tHex-Hep). No elongation was found at HepII, instead HepI was elongated by a HexNAc-Hex-Hex-NAc-Hex-Hex unit. This was evidenced by ions *m*/*z* 2106.9, 1903.0, 1658.0 and 1453.9 due to losses corresponding to a terminal HexNAc-Hex-HexNAc-Hex unit. When the ion at *m*/*z* 1658.0 was further fragmented in a MS^3 experiment, the ions *m*/*z* 1454.5, 1250.1 and 737.7 due to consecutive losses of a Hex-Hex-Hep-*An*Kdo-ol unit confirmed the substitution at HepI (Scheme 2).

3.2.2. Characterization of OS-1 by NMR spectroscopy. The ^1H NMR spectrum was assigned using chemical shift correlation techniques (COSY and TOCSY experiments) and the chemical shift data are presented in Table 6. Subspectra corresponding to the individual glycosyl residues were identified on the basis of spin-connectivity pathways delineated in the ^1H chemical shift correlation maps, the chemical shift values, and the vicinal coupling constants. The chemical shift data are consistent with each D-sugar residue being present in the pyranosyl ring form. Further evidence for this conclusion was obtained from NOE data (Table 7) which also served to confirm the anomeric configurations of the

Table 4
Product ions observed in the MS^2 and MS^3 spectra for the various dephosphorylated and permethylated glycoforms in NTHi strain 162 and proposed fragmentation

Glycoform	Parent ion (*m/z*) MS^1	Product ion (*m/z*) MS^2	Neutral loss	Product ion (*m/z*) MS^3	Neutral loss
Hex1 [a]	1264.3	1045.6	tHex-	797.4	-Hep-
				783.4	tHep-
				767.3	-*An*Kdo-ol
				533.3	-(−)Hep-*An*Kdo-ol
		1001.6	tHep-		
		985.5	-*An*Kdo-ol		
		797.5	tHex-Hep-		
		753.5	tHep-Hep-		
		737.4	Hep-*An*Kdo-ol	519.3	tHex-
				489.2	-Hep-
				270.9	tHex-Hep-
Hex2	1468.1	1249.7	tHex-	1131.5	tHex-
				1001.5	-Hep-
				783.5	tHex-Hep-
				753.5	-Hep-Hep-
				737.4	-(−)Hep-*An*Kdo-ol
				568.9	n.r.
		1189.5	-*An*Kdo-ol		
		1001.6	tHex-Hep-		
		753.5	tHex-Hep-Hep-		
		737.5	tHex-Hep-*An*Kdo-ol	519.3	tHex-
				507.2	n.r.
				489.2	-Hep-
				271.0	tHex-Hep-
Hex3	1672.0	1453.7	tHex-		
		1249.7	tHex-Hex-	1031.7	tHex-
				1001.5	-Hep-
				753.4	-Hep-Hep-
		1206.7	n.r.		
		1001.6	tHex-Hex-Hep-		
		941.5	tHex-Hep-*An*Kdo-ol	723.4	tHex-
				693.4	-Hep-
				578.4	n.r.
				519.3	tHex-Hex-
				445.1	-Hep-Hep-
		753.5	tHex-Hex-Hep-Hep-		
		693.4	tHex-Hep(Hep)-*An*Kdo-ol		
Hex4	1875.9	1657.8	tHex-		
		1453.8	tHex-Hex-		
		1249.7	tHex-Hex-Hex-		
		1145.6	tHex-Hep-*An*Kdo-ol	927.5	tHex-
				897.5	-Hep-
				723.3	tHex-Hex-
				649.3	-Hep-Hep-
				619.3	n.r.
		1001.6	tHex-Hex-Hex-Hep-		
		897.5	tHex-Hep(Hep)-*An*Kdo-ol		
		753.4	tHex-Hex-Hex-Hep-Hep-		
Hex5	2121.6	1904.0	tHex-		
		1861.9	tHexNAc-		
		1658.0	tHexNAc-Hex-		
		1454.0	tHexNAc-Hex-Hex-		

Table 4 (*Continued*)

Glycoform	Parent ion (*m*/*z*) MS[1]	Product ion (*m*/*z*) MS[2]	Neutral loss	Product ion (*m*/*z*) MS[3]	Neutral loss
		1391.2	tHex-Hep-*An*Kdo-ol	1143.5	-Hep-
				1132.3	tHexNAc-
				928.4	tHexNAc-Hex-
				895.9	-Hep-Hep-
				865.1	n.r.
		1250.1	tHexNAc-Hex-Hex-Hex-	1032.1	tHex-
				754.4	-Hep-Hep-
				520.0	tHex-Hep-*An*Kdo-ol
		1143.4	tHex-Hep(Hep)-*An*Kdo-ol		
		1002.5	tHexNAc-Hex-Hex-Hex-Hep-		
Hex6 [b]	2365.2	2215.5	n.r.		
		2148.5	tHex	1900.6	-Hep-
				1441.1	tHexNAc-Hex-Hex-NAc-
		2120.8	n.r.		
		2106.9	tHexNAc-		
		1903.0	tHexNAc-Hex-	1658.5	-HexNAc
				1652.7	n.r.
				1437.2	tHex-Hep-
				1192.9	-HexNAc-; tHex-Hep-
		1900.6	tHex-Hep-		
		1658.0	tHexNAc-Hex-HexNAc-	1454.5	-Hex-
				1440.1	tHex-
				1250.1	-Hex-Hex-
				1192.2	tHex-Hep-
				944.2	tHex-Hep-Hep-
				737.7	-Hex-Hex-Hep-*An*-Kdo-ol
		1453.9	tHexNAc-Hex-HexNAc-Hex-		
		1192.3	n.r.		
		944.4	n.r.		

Given are ions with more than 5% abundance and of significant structural information; n.r., not rationalized. tHex- represents loss of a terminal hexose (Me_4-Hex), -Hex-represents loss of a substituted hexose (Me_3-Hex), -(−)Hep- represents loss of a branched heptose (Me_3-Hep), -*An*Kdo-ol represents loss of reduced anhydro-Kdo (Me_4-*An*Kdo-ol), etc.

[a] Only present in OS-2.

[b] Only present in OS-1.

linkages and the monosaccharide sequence. The Hep ring systems were identified on the basis of the small $J_{1,2}$-values and their α-configurations were confirmed by the occurrence of single intraresidue NOE between the respective H-1 and H-2 resonances. Several signals for methylene protons of *An*Kdo-ol were observed in the COSY and TOCSY spectra in the region 2.16–1.85ppm. This is due to the fact that several anhydro-forms of Kdo are formed during the hydrolysis as observed earlier.[12]

The structures of the major glycoforms in OS-1 were determined by examining the ^{1}H-NMR spectrum in detail. The characteristic signal for the methyl groups of *P*Cho was observed at δ 3.24. Anomeric resonances of HepI-HepIII were identified at δ 5.03–5.13, 5.63 and 5.11, respectively. Subspectra corresponding to GlcI, GlcII, Gal_I, Gal_II and GalNAc in the major Hex5 glycoform were identified in the 2D COSY and TOCSY spectra at δ 4.51, 4.68, 4.51, 4.92 and 4.63, respectively. From the downfield shifted H-6_A,6_B signals of GlcI at δ 4.30, it was concluded that this residue was substituted with *P*Cho at that position, which was in agreement with previous CE-ESIMS/MS analyses.[29] Interresidue NOE connectivities (Table 7) between proton pairs GalNAc H-1/Gal_II H-3, Gal_II H-1/GlcII H-4, GlcII H-1/HepIII H-1,2 established the sequence of a globote-

Table 5
Hex1–Hex6 isomeric glycoforms observed in non-typeable *H. influenzae* strain 162 as identified by multiple tandem ESIMS (ESIMS^n)

Hex1	Hex-Hep-Kdo | Hep | Hep	Hep-Kdo | Hep | Hex-Hep
Hex2	Hex-Hep-Kdo | Hep | Hex-Hep	
Hex3	Hex-Hep-Kdo | Hep | Hex-Hex-Hep	
Hex4	Hex-Hep-Kdo | Hep | Hex-Hex-Hex-Hep	
Hex5	Hex-Hep-Kdo | Hep | HexNAc-Hex-Hex-Hex-Hep	
Hex6	HexNAc-Hex-HexNAc-Hex-Hex-Hep-Kdo | Hep | Hex-Hep	

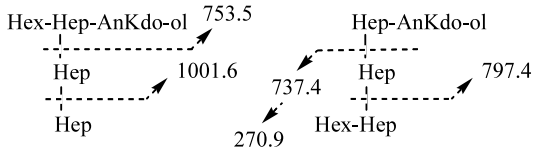

Scheme 1. Fragmentation pattern of the Hex1 glycoforms.

traose (β-D-Gal*p*NAc-(1→3)-α-D-Gal*p*-(1→4)-β-D-Gal*p*-(1→4)-β-D-Glc*p*-(1→) unit linked to HepIII. In addition, interresidue NOE connectivities between proton pairs GlcI H-1/HepI H-4,6, HepIII H-1/HepII H-2, HepII H-1/HepI H-3 confirmed the presence of the common inner-core triheptosyl moiety of *H. influenzae* substituted by a β-D-Glc*p* residue at HepI. From the combined data, it could thus be concluded that the major Hex5 glycoform has structure **2**. In accord with ESIMS, MS^n, and methylation analysis data, the structures of the Hex4 and Hex3 glycoforms are assigned to those having the globotriose (α-D-Gal*p*-(1→4)-β-D-Gal*p*-(1→4)-β-D-Glc*p*-(1→) and lactose (β-D-Gal*p*-(1→4)-β-D-Glc*p*-(1→), respectively, linked to HepIII. We have previously identified the globotetraose glycoform in *H. influenzae* strain Rd[12] and established the genetic basis for its assembly.[5] As found earlier, Gly partly substitutes all glycoforms at HepII and Kdo as evidenced from CE-ESIMS/MS.[29]

4. Discussion

As a part of our ongoing studies on the role of *H. influenzae* LPS in disease pathogenesis and in eliciting protective immune responses, we have undertaken a systematic analysis of LPS from a genetically diverse set of NTHi strains obtained from an epidemiological study of otitis media in Finland.[13] Structural studies have revealed that every strain investigated to date[12–21] elaborates LPS containing the conserved triheptosyl inner-core moiety (structure **3**).

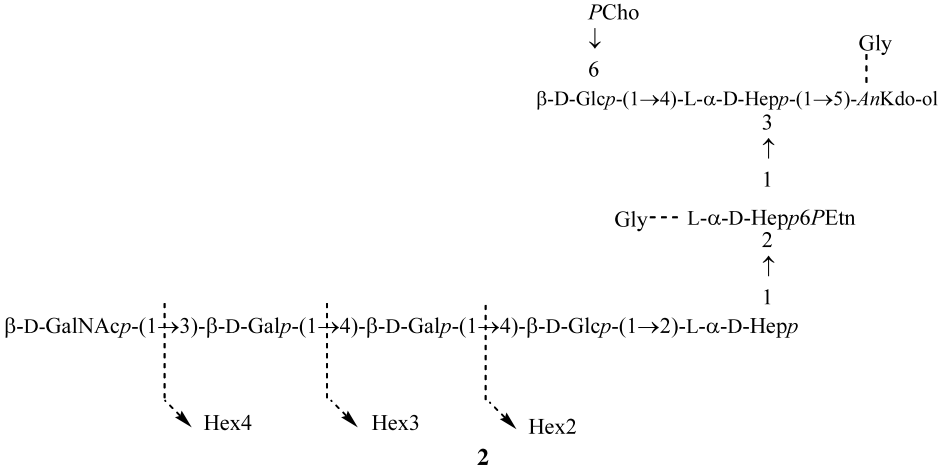

2

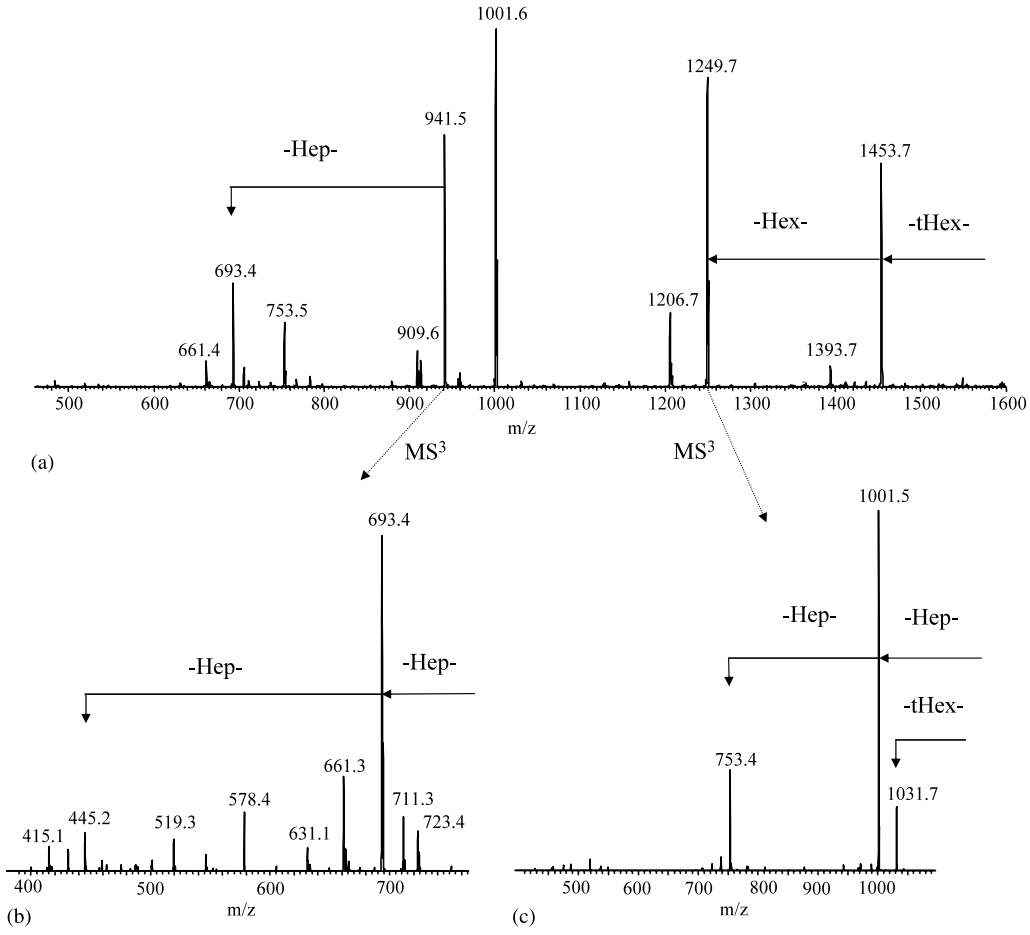

Fig. 2. MS^2 and MS^3 mass spectra derived from the Hex3 glycoform and its proposed fragmentation pattern. (A) Product ion spectrum of $[M+Na]^+$ *m/z* 1671.9; (B) MS^3 spectrum of fragment ion *m/z* 941.5; (C) MS^3 spectrum of fragment ion *m/z* 1249.7.

*PP*Etn
↓
4
R^1→4)-L-α-D-HepI*p*-(1→5)-α-Kdo*p*-(2→6)-Lipid A
3
↑
1
R^2→3)-L-α-D-HepII*p*6←*P*Etn
2
↑
1
R^3→2/3)-L-α-D-HepIII*p*

3 (R^1, R^2, R^3 = H or sugar residues)

HepI has been found to be substituted by a β-D-Glc*p* (R^1) in all strains investigated and this residue can be further substituted by glycoses[16,17,20,21,24] and/or phosphocholine.[22] There is no chain extension from HepII in strain Rd, however, in type b[17,18] and several NTHi strains,[19–21] this heptose is substituted by an α-D-Glc*p* residue (R^2) which can provide a point for further chain extension. HepIII has been found, depending on the strain, to be substituted at either the O2 or O3 position

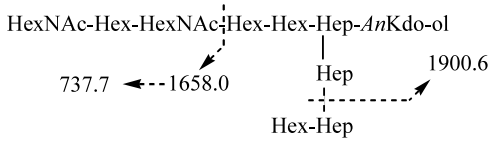

Scheme 2. Fragmentation pattern of the Hex6 glycoform.

Table 6
^{1}H NMR chemical shifts for OS-1 derived from NTHi strain 162

Sample	Residue	Glycose unit	H–1	H-2	H-3	H-4	H-5	H-6$_A$	H-6$_B$	H-7$_A$	H-7$_B$
OS-1	HepI	→3,4)-L-α-D-Hep*p*-(1→	5.03–5.13[a] (n.r.)	3.98–4.06[a]	3.98–4.06[a]	4.23[b]	–[c]	4.14[b]		–	–
	HepII	→ 2)-L-α-D-Hep*p*-(1→ 6 ↑ *P*Etn	5.63 (n.r.)	4.34	3.95	–	–	4.56		3.70	3.88
	HepIII	→2)-L-α-D-Hep*p*(1→	5.11 (n.r.)	4.26	3.97	–	–	–		–	–
	GlcI	β-D-Glcp-(1→ 6 ↑ *P*Cho	4.51 (7.4)	3.38	3.46	3.61	3.53	4.18	4.28		
	GlcII	→4)-β-D-Glc*p*-(1→	4.68 (7.6)	3.36	3.70	3.70	3.70	4.00	3.82		
	Gal_I	→4)-β-D-Gal*p*-(1→	4.51 (7.6)	3.60	3.75	4.04	3.70[d]	3.88[d]	3.86[d]		
	Gal_II	→3)-α-D-Gal*p*-(1→	4.92 (3.6)	3.88	3.96	4.24	–	–	–		
	GalNAc	β-D-GalNAc*p*-(1→	4.63	3.75	3.96	4.18	–	–	–		
	*P*Etn		4.14	3.28							
	*P*Cho		4.39	3.70							

Data were recorded in D_2O at 25 °C. $^3J_{H,H}$ values for anomeric ^{1}H resonances (H-1) are given in parentheses; n.r., not resolved (small coupling). The signal corresponding to *P*Cho methyl protons was observed at 3.24 ppm. Pairs of deoxyprotons of reduced, *An*Kdo were identified in the DQF-COSY at 2.16–1.85 ppm.

[a] Several signals were observed for HepI and HepII due to heterogeneity in the *An*Kdo moiety.

[b] H-4/H-6 of HepI are observed by NOE from H-1 of GlcI.

[c] –, not obtained.

[d] Tentative assignment from NOE data.

Table 7
Proton NOE data for OS-1 derived from LPS of NTHi strain 162

Anomeric proton HepI	Observed proton	
	Intraresidue NOE	Interresidue NOE
HepI	H-2	n.r.[a]
HepII	H-2	H-3 of HepI; H-1 of HepIII
HepIII	H-2	H-1, H-2 of HepII
GlcI	H-3, H-5	H-4, H-6 of HepI
GlcII	H-3, H-5	H-1, H-2 of HepIII
Gal_I	H-3, H-5	H-4 of GlcII
Gal_II	H-2	H-4 of Gal_I
GalNAc	H-3	H-3 of Gal_II

Measurements were made from NOESY experiments.

[a] n.r., not rationalized.

(R^3) by a β-D-Gal*p*[17,18,20,21] or oligosaccharides extending from a β-D-Glc*p*.[12,14,16,19] Prominent non-carbohydrate substituents are phosphate (*P*), pyrophosphoethanolamine (*PP*Etn), phosphoethanolamine (*P*Etn), phosphocholine (*P*Cho), acetate (Ac) and glycine (Gly). In the present investigation, it was found that NTHi strain 162 can express the major biantennary LPS oligosaccharide structures that are present in *H. influenzae* strain Rd.[12] Thus, HepI is substituted at O-4 by a *P*Cho→6)-β-D-Glc*p* unit (R^1), with chain elongation in the major glycoforms from O-2 of HepIII; a Hex5 glycoform that carries a globotetraose side-chain (R^3 = β-D-Gal*p*NAc-(1→3)-α-D-Gal*p*-(1→4)-β-D-Gal*p*-(1→4)-β-D-Glc*p*) from which sequentially truncated Hex4 and Hex3 glycoforms contain globotriose (R^3 = α-D-Gal*p*-(1→4)-β-D-Gal*p*-(1→4)-β-D-Glc*p*) and lactose (R^3 = β-D-Gal*p*-(1→4)-β-D-Glc*p*) chains, respectively. Strain Rd is an *H. influenzae* type d capsular strain which was chosen for complete genomic analysis.[3] We have recently identified the glycosyltransferases involved in the assembly of the globotetraose side chain in a capsular deficient mutant of the Rd strain.[5] The *lpsA* gene was shown to be involved in the addition of the β-D-Glc*p* residue in a (1→2)-linkage to initiate chain extension from HepIII. Phase variable genes, *lic2A* and *lgtC* encode the galactosyltransferases involved in sequential addition of the β-1,4-linked D-Gal*p* (Lic2A) and α-(1→4)-linked D-Gal*p* (LgtC) residues of the globotriose unit. Addition of a β-(1→3)-linked D-Gal*p*NAc unit to the terminal α-D-Gal*p* residue of the globotriose, mediated by *lgtD*, gives rise to the fully assembled globotetraose unit.[5] The presence of these

genes in NTHi strain 162 has been confirmed by a comparative genomics analysis (Hood and co-workers, unpublished results). It is noteworthy that Hex2 and Hex5 are the major LPS glycoforms observed in NTHi strain 162 suggesting that phase variation of *lic2A* controls further chain extension from HepIII with *lgtC* being predominately phased 'on'. Sialylated Hex3 glycoforms were also identified by ESIMS in strain 162. We have shown that the phase variable gene, *lic3A* encodes a sialyltransferase that mediates addition of CMP-NeuAc to lactose in Hex3 glycoforms ($R^3 = \beta$-D-Gal*p*-(1→4)-β-D-Glc*p*) of several *H. influenzae* strains.[23] Sialylated glycoforms have been identified in most NTHi clinical isolates.[34] A disialylated structural motif (α-NeuAc-(2→8)-α-NeuAc-(2→3)-β-D-Gal*p*-(1→4)-β-D-Glc*p*) has also been observed in NTHi 375[13] but not in strain Rd. Recently, we demonstrated that expression of sialylated glycoforms by NTHi, including strain 162, is an essential virulence determinant in experimental otitis media.[25]

A strategy for analysis of permethylated oligosaccharides by ESIMS/MS on triple-quadrupole instruments was introduced by Reinhold and co-workers in the early 1990s and then combined with the use of a quadrupole ion trap mass spectrometer (ITMS), an instrument that provides multistage MS/MS (MS^n).[27,28] By using the approach described herein on dephosphorylated oligosaccharide samples, we were able to obtain information on oligosaccharide sequence giving an isomeric profile of LPS glycoforms. This is a rapid and sensitive approach that enables detection of isomeric glycoforms that are present in low abundance. Application of this approach has provided clear evidence that the NTHi 162 Hex2 to Hex5 LPS glycoforms are only elaborated as the isomers indicated in structure **2**. In addition, minor Hex1 glycoforms were identified that exist as two isomers: one, representative of the inner-core structural unit of *H. influenzae* having a glucose residue linked to HepI (structure **3**: $R^1 = \beta$-D-Glc*p*; R^2,R^3 = H); and, another having HepI monosubstituted by HepII (structure **3**: R^1, R^2 = H; $R^3 = \beta$-D-Glc*p*). A minor Hex6 glycoform detected by $ESIMS^n$ showed a completely different pattern of oligosaccharide chain extension from that of the major population of glycoforms. Instead of being substituted by a single glucose residue at HepI, the Hex6 glycoform was elongated by a HexNAc-Hex-HexNAc-Hex-Hex chain on HepI (R^1) and a single hexose residue on HepIII (R^3). We have recently identified this LPS structural motif in several NTHi strains (Schweda and co-workers, unpublished results). It is particularly noteworthy that truncated analogues of this isomeric glycoform are not detectable in any of the strains in which it is observed. Moreover, sialylated lacto-*N*-neotetraose, having a related sequence, was recently identified in strain Rd as a chain extension from HepI (structure **3**: $R^1 = \alpha$-NeuAc-(2→3)-β-D-Gal*p*-(1→4)-β-D-Glc*p*NAc-(1→3)-β-D-Gal*p*-(1→4)-β-D-Glc*p*).[24] The genetic basis for the biosynthesis of these extended oligosaccharide chains from HepI of the inner core template in *H. influenzae* LPS is currently under investigation in our laboratories.

LPS oligosaccharide epitopes can provide a source of protective antigens against *H. influenzae* when they are presented to the host immune system in an appropriate fashion, for example, as a protein-conjugate. Human antibodies and mouse monoclonal antibodies against certain NTHi LPS have been shown to have bactericidal activity in vitro.[35,36] Recent studies have indicated that immunization with LPS-based conjugates can reduce the incidence of NTHi-induced otitis media due to the homologous strain in an animal model[37] and conjugate induced LPS antibodies can confer immunity to NTHi by binding to its LPS, likely through a mechanism involving inhibition of NTHi adherence.[38] A key concept in choosing LPS as vaccine candidate is that these surface expressed carbohydrate antigens may possess oligosaccharide epitopes that are genetically and physiologically stable, conserved across the range of clinically relevant strains, and accessible to host clearance mechanisms. Our structural studies of NTHi strain 162 establish that this strain elaborates the triheptosyl inner-core unit that is found in every *H. influenzae* strain investigated, providing a template for substitution by variable outer-core oligosaccharide epitopes. These structural motifs have been identified in a number of other strains including the genome strain Rd.[12–16] NTHi strain 162 elaborates biantennary structures with chain extensions occurring from HepI and HepIII only, a structural feature that has been subsequently shown by genomic analysis to be a common motif among a genetically diverse set of clinical isolates of NTHi (Hood and co-workers, unpublished). These structural motifs could provide the basis for a vaccine strategy against the known disease causing NTHi isolates.

Acknowledgements

The authors thank Juhani Eskola and the members of the Finnish Otitis Media Study Group at the National Public Health Institute in Finland for the provision of the NTHi strain used in this study. Mary Deadman is acknowledged for culture of NTHi strain 162. Financial assistance from Aventis Pasteur and the Karolinska Institutet (KI-fonder) is greatfully acknowledged.

References

1. Teele, D. W.; Klein, J. O.; Rosner, B.; Bratton, L.; Fisch, G. R.; Mathieu, O. R.; Porter, P. J.; Starobin, S. G.;

Tarlin, L. D.; Younes, R. P. *J. Am. Med. Assoc.* **1996**, *249*, 1026–1029.
2. Kilpi, T.; Herva, E.; Kaijalainen, T.; Syrjanen, R.; Takala, A. K. *Pediatr. Infect. Dis. J.* **2001**, *20*, 654–662.
3. Fleischmann, R.; Adams, M.; White, O.; Clayton, R.; Kirkness, E.; Kerlavage, A.; Bult, C.; Tomb, J.; Dougherty, B.; Merrick, J.; McKenney, K.; Sutton, G. G.; FitzHugh, W.; Fields, C. A.; Gocayne, J. D.; Scott, J. D.; Shirley, R.; Liu, L. I.; Glodek, A.; Kelley, J. M.; Weidman, J. F.; Phillips, C. A.; Spriggs, T.; Hedblom, E.; Cotton, M. D.; Utterback, T.; Hanna, M. C.; Nguyen, D. T.; Saudek, D. M.; Brandon, R. C.; Fine, L. D.; Fritchman, J. L.; Fuhrmann, J. L.; Geoghagen, N. S.; Gnehm, C. L.; McDonald, L. A.; Small, K. V.; Fraser, C. M.; Smith, H. O.; Venter, J. C. *Science* **1995**, *269*, 496–512.
4. Hood, D. W.; Deadman, M. E.; Allen, T.; Masoud, H.; Martin, A.; Brisson, J. R.; Fleischmann, R.; Venter, J. C.; Richards, J. C.; Moxon, E. R. *Mol. Microbiol.* **1996**, *22*, 951–965.
5. Hood, D. W.; Cox, A. D.; Wakarchuk, W. W.; Schur, M.; Schweda, E. K. H.; Walsh, S. L.; Deadman, M. E.; Martin, A.; Moxon, E. R.; Richards, J. C. *Glycobiology* **2001**, *11*, 957–967.
6. Kimura, A.; Hansen, E. J. *Infect. Immun.* **1986**, *51*, 69–79.
7. Weiser, J. N.; Williams, A.; Moxon, E. R. *Infect. Immun.* **1990**, *58*, 3455–3457.
8. Weiser, J. N. *J. Infect. Dis.* **1993**, *168*, 672–680.
9. Weiser, J. N.; Maskell, D. J.; Butler, P. D.; Lindberg, A. A.; Moxon, E. R. *J. Bacteriol.* **1990**, *172*, 3304–3309.
10. Hood, D. W.; Deadman, M. E.; Jennings, M. P.; Bisercic, M.; Fleischmann, R. D.; Venter, J. C.; Moxon, E. R. *Proc. Natl. Acad. Sci. USA* **1996**, *93*, 11121–11125.
11. Jarosik, G. P.; Hansen, E. J. *Infect. Immun.* **1994**, *62*, 4861–4867.
12. Risberg, A.; Masoud, H.; Martin, A.; Richards, J. C.; Moxon, E. R.; Schweda, E. K. H. *Eur. J. Biochem.* **1999**, *261*, 171–180.
13. Hood, D. W.; Makepeace, K.; Deadman, M. E.; Rest, R. F.; Thibault, P.; Martin, A.; Richards, J. C.; Moxon, E. R. *Mol. Microbiol.* **1999**, *33*, 679–692.
14. Månsson, M.; Hood, D. W.; Li, J.; Richards, J. C.; Moxon, E. R.; Schweda, E. K. H. *Eur. J. Biochem.* **2002**, *269*, 808–818.
15. Rahman, M. M.; Gu, X.-X.; Tsai, C.-M.; Kolli, V. S. K.; Carlson, R. W. *Glycobiology* **1999**, *9*, 1371–1380.
16. Månsson, M.; Hood, D. W.; Moxon, E. R.; Schweda, E. K. H. *Eur. J. Biochem.* **2003**, *270*, 610–624.
17. Phillips, N. J.; Apicella, M. A.; Griffiss, J. M.; Gibson, B. W. *Biochemistry* **1993**, *32*, 2003–2012.
18. Masoud, H.; Moxon, E. R.; Martin, A.; Krajcarski, D.; Richards, J. C. *Biochemistry* **1997**, *36*, 2091–2103.
19. Månsson, M.; Bauer, S. H. J.; Hood, D. W.; Richards, J. C.; Moxon, E. R.; Schweda, E. K. H. *Eur. J. Biochem.* **2001**, *268*, 2148–2159.
20. Schweda, E. K. H.; Li, J.; Moxon, E. R.; Richards, J. C. *Carbohydr. Res.* **2002**, *337*, 409–420.
21. Cox, A. D.; Masoud, H.; Thibault, P.; Brisson, J.-R.; van der Zwan, M.; Perry, M. B.; Richards, J. C. *Eur. J. Biochem.* **2001**, *268*, 5278–5286.
22. Schweda, E. K. H.; Brisson, J.-R.; Alvelius, G.; Martin, A.; Weiser, J. N.; Hood, D. W.; Moxon, E. R.; Richards, J. C. *Eur. J. Biochem.* **2000**, *267*, 3902–3913.
23. Hood, D. W.; Cox, A. D.; Gilbert, M.; Makepeace, K.; Walsh, S.; Deadman, M. E.; Cody, A.; Martin, A.; Månsson, M.; Schweda, E. K. H.; Brisson, J.-R.; Richards, J. C.; Moxon, E. R.; Wakarchuk, W. W. *Mol. Microbiol.* **2001**, *39*, 341–350.
24. Cox, A. D.; Hood, D. W.; Martin, A.; Makepeace, K.; Deadman, M. E.; Li, J.; Brisson, J.-R.; Moxon, E. R.; Richards, J. C. *Eur. J. Biochem.* **2002**, *269*, 4009–4019.
25. Bouchet, V.; Hood, D. W.; Li, J.; Brisson, J.-R.; Randle, G. A.; Martin, A.; Li, Z.; Goldstein, R.; Schweda, E. K. H.; Pelton, S. I.; Richards, J. C.; Moxon, E. R. *Proc. Natl. Acad. Sci. USA*. **2003**, *100*, 8898–8903.
26. Cody, A. J.; Field, D.; Feil, E. J.; Stringer, S.; Deadman, M. E.; Tsolaki, A. G.; Gratz, B.; Bouchet, V.; Goldstein, R.; Hood, D. W.; Moxon, E. R. *Infection, Genetics and Evolution*. **2003**, *3*, 57–60.
27. Sheeley, D. M.; Reinhold, V. N. *Anal. Chem.* **1998**, *70*, 3053–3059.
28. Mühlecker, W.; Gulati, S.; McQuilien, D. P.; Ram, S.; Rice, P. A.; Reinhold, V. N. *Glycobiology* **1999**, *9*, 157–171.
29. Li, J.; Bauer, S. H. J.; Månsson, M.; Moxon, E. R.; Richards, J. C.; Schweda, E. K. H. *Glycobiology* **2001**, *11*, 1009–1015.
30. Holst, O.; Brade, L.; Kosma, P.; Brade, H. *J. Bacteriol.* **1991**, *173*, 1862–1866.
31. Sawardeker, J. S.; Sloneker, J. H.; Jeanes, A. *Anal. Chem.* **1965**, *37*, 1602–1604.
32. Blakeney, A. B.; Stone, B. A. *Carbohydr. Res.* **1985**, *140*, 319–324.
33. Gerwig, G. J.; Kamerling, J. P.; Vliegenthart, J. F. G. *Carbohydr. Res.* **1979**, *77*, 1–7.
34. Bauer, S. H. J.; Månsson, M.; Hood, D. W.; Richards, J. C.; Moxon, E. R.; Schweda, E. K. H. *Carbohydr. Res.* **2001**, *335*, 251–260.
35. Barenkamp, S. J.; Bodor, F. F. *Pediatr. Infect. Dis. J.* **1990**, *9*, 333–339.
36. Ueyama, T.; Gu, X. X.; Tsai, C. M.; Karpas, A. B.; Lim, D. J. *Clin. Diagn. Lab. Immunol.* **1999**, *6*, 96–100.
37. Gu, X.-X.; Tsai, C.-M.; Ueyama, T.; Barenkamp, J.; Robbins, J. B.; Lim, D. J. *Infect. Immun.* **1996**, *64*, 4047–4053.
38. Sun, J.; Chen, J.; Cheng, Z.; Robbins, J. B.; Battey, J. F.; Gu, X. X. *Vaccine* **2000**, *18*, 1264–1272.